An Integrated Computer Model with Applications for Austenite-to-Ferrite Transformation during Hot Deformation of Nb-Microalloyed Steels

JANUSZ MAJTA, ANNA K. ZUREK, MARK COLA, PAT HOCHANADEL, and MACIEJ PIETRZYK

This work presents an austenite decomposition model, based on the thermodynamics of the system and diffusion-controlled nucleation theory, to predict the evolution of microstructure during hot working of niobium-microalloyed steels. The differences in microstructural development of hot-deformed microalloyed steel in the single-phase austenite and two-phase (austenite + ferrite) regions have been effectively described using an integrated computer modeling process. The complete model presented here takes into account the kinetics of recrystallization, recrystallized austenite grain size, precipitation, phase transformation, and the resulting ferrite structure. After considering existing austenite decomposition models, we decided that the method adopted in the present work relies on isothermal transformation kinetics and the principle-of-additivity rule. The thermomechanical part of the modeling process was carried out using the finite-element method. Experimental results at different temperatures, strain rates, and strain levels were obtained using a Gleeble thermomechanical simulator. A comparison of results of the model with experiments shows good agreement.

I. INTRODUCTION

HOT working of low-carbon steels is generally carried out over a wide range of conditions in which the deformation-temperature range of the single-phase austenite is stable. However, it is well established that a new and attractive combination of properties can be obtained when the final product has a structure that comes from deformation performed in the two-phase (austenite + ferrite) region. In steels hot worked in the two-phase region, the inhomogeneity of the microstructure and the resulting variations in mechanical behavior constitute major difficulties. It is well known that the most effective and powerful tool to control such complicated deformation conditions is computer modeling. One of the most basic elements of the thermomechanical treatment of microalloyed steels is the transformation from deformed, unrecrystallized austenite.[1] Such austenite contains an enhanced number of ferrite nucleation sites; *i.e.*, dislocations, deformation bands, and deformation twins. The increase in nucleation density leads to significant ferrite grain refinement. Usually, the ferrite nucleation process starts on the austenite grain-boundary sites. When ferrite nucleation sites change from grain boundaries to intragranular sites during accelerated cooling, for example, the resulting microstructure begins to be refined, but is also more inhomogeneous. To analyze such a complex transformation behavior, a versatile model of the transformation kinetics is needed.

The modeling of austenite decomposition under the previously mentioned conditions has been discussed in several recent publications.[2–10] In the present work, the austenite decomposition is described based on the assumption that nucleation of transformed ferrite is a probabilistic phenomenon and occurs mostly on the surface of grain boundaries. Because the steel investigated is a microalloyed grade, attention was mostly focused on the austenite-to-ferrite transformation. Assuming that for low-carbon steels the ferrite phase is the major element of the final structure, the formation of pearlite was not studied in this model.

In general, a proper γ/α transformation model should be constructed in terms of three basic parameters: the transformation start temperature (T_s), the kinetics of austenite decomposition (dX/dt), and the latent heat generated during transformation (Q). Therefore, these parameters should be contained in the complete model. Because of the difficulties in determining the isothermal data for low-carbon microalloyed steels that have very short transformation times, the value of a well-verified computer model cannot be overemphasized, especially as the model is applied to intercritical or warm-rolling processes.

II. STATE-OF-THE-ART OF AUSTENITE DECOMPOSITION MODELING

A. *Comparison of Austenite-Ferrite Transformation Models Employed in the Analysis of Microalloyed Steels*

Although the first mathematical model of phase transformation during continuous cooling was presented by Kirkaldy[3] almost 30 years ago, only recently has modeling of the phase transformation process become the target of extensive research. It is possible to distinguish at least five very specific approaches that are used in the modeling of austenite decomposition. Most of them are based on a common Avrami–Johnson–Mehl equation.

Suehiro *et al.*[4,5] proposed the first of the transformation models based on general metallurgical theories with a number of empirical parameters. They eliminated the time term

JANUSZ MAJTA, Professor, and MACIEJ PIETRZYK, Professor, are with the Metallurgy and Materials Science Department, University of Mining and Metallurgy, 30-059 Krakow, Poland. ANNA K. ZUREK, MARK COLA, and PAT HOCHANADEL, Staff Members, are with Materials Science and Technology, Los Alamos National Laboratory, Los Alamos, NM 87545.

Manuscript submitted November 5, 1999.

in the Avrami equation after differentiation, based on the assumption of the additivity rule of the transformation product at various temperatures. Taking into account that the transformation progresses at a later stage according to the site-saturation condition, they formulated separate equations for nucleation and growth and for site saturation. The solutions proposed here for model calibration require extensive experimentation. However, the attractive feature of this model is that it can be used without constructing time-temperature-transformation diagrams, which require enormous time and labor and are very difficult to obtain for Nb-microalloyed steels. This model was also analyzed in several other articles (Senuma *et al.*[6] and Torizuka *et al.*[7]).

In the second model, proposed by Yoshie *et al.*,[8] the ferrite transformation was formulated for grain-boundary ferrite and intragranular ferrite separately. The nucleation rates of each of the aforementioned were described as a function of the concentration of microalloying elements (Nb, V, and Ti) in solution, temperature, and average dislocation density. They assumed that the average dislocation density represents the effect of all the lattice defects after deformation in the nonrecrystallization-temperature region. Further, using the average dislocation density, they described the austenite-to-ferrite transformation kinetics.

The next model was proposed by Choquet *et al.*[9] This is clearly an empirical model. From consideration of the shape of the experimental kinetics curves in continuous cooling conditions, an equation for the transformation rate was derived.

More recently, Boyadijiev *et al.*[11,12] and Umemoto *et al.*[13,14] proposed a model for predicting the phase transformation during cooling from work-hardened austenite. They used the principles of physical metallurgy and basic transformation kinetics equations, assuming (similar to Suehiro) that continuous cooling is the sum of short-time isothermal holdings at successive temperatures. This model seems to have a well-formulated theoretical background. Unfortunately, because of the number of experimentally obtained parameters, this model's calibration process also is very cumbersome in the case of Nb-microalloyed steels.

Finally, the approach for considering austenite structure proposed originally by Umemoto[15] should be mentioned. The author developed a simple equation for isothermal transformation kinetics that also justifies the extension of Scheil's additivity rule to the whole transformation range. The most important effect on microstructure development in the steel has the effect of a niobium addition; therefore, this problem is discussed in detail in the next two sections of the present work.

B. *Transformation Start Temperature*

It is widely recognized that hot deformation of austenite in the absence of concurrent recrystallization strongly influences the austenite-to-ferrite phase-transformation kinetics during cooling. It can be contended that thermomechanical processing accelerates the onset of γ/α transformation (raises T_s), but retards the progress of transformation. Therefore, the first element in the characterization of microstructure development is the austenite-to-ferrite transformation start temperature (T_s).

Several ideas for calculating the transformation start temperature were proposed in the literature. The most popular in engineering practice is that suggested by Ouchi *et al.*,[16]

$$T_s = 910 - 310\text{C} - 80\text{Mn} - 20\text{Cu} - 15\text{Cr} - 55\text{Ni} - 80\text{Mo} + 0.35(t - 8) \quad [1]$$

where T_s is the transformation start temperature (in degrees Celsius), and t is the plate thickness (in millimeters).

This equation makes it possible to calculate the γ/α transformation start temperature on the basis of chemical composition and plate thickness. However, it should be mentioned that Eq. [1] is applicable beyond a 50 pct reduction in the unrecrystallized austenite region when T_s tends to plateau. Although this formula is often applied, the results obtained in this way are relatively scattered. A more complex correlation between transformation start temperature and process parameters was proposed by Piette and Perdrix.[17]

$$T_s = A - B(1 + f(\text{Nb})g(\varepsilon_a)h(D_\gamma)C_r^{0.5} \quad [2]$$

where A and B are constants depending on chemical composition, C_r is the cooling rate, D_γ is the austenite grain size, and ε_a is the retained strain (in unrecrystallized austenite).

In this case, the particular hot-working condition has been taken into consideration. The only question is, what are the meanings of the functions f, g, and h? Nevertheless, the influence of the most-important elements necessary for the start of the transformation process is reflected.

In the present work, we suggest that the transformation start temperature can be calculated reasonably well according to the following formula:[18]

$$T_s = A - 19C_r^{0.481} - 0.5 \exp\left(\frac{0.042D_\gamma + 7.8}{(2.11 + \varepsilon_a)^{1.35}}\right) \quad [3]$$

where A is a constant that depends only on the steel chemical composition (in the present work, $A = 830$), C_r is cooling rate, D_γ is the austenite grain size, and ε_a is the retained strain (in unrecrystallized austenite).

A literature database[16,19,20–23] and our own isothermal experiments[24,25] were used to determine the parameters in Eq. [3]. There are several ways to explain what roles particular elements play in Eq. [3]. The purpose of increasing the cooling rate and/or the austenite grain size is to lower the transformation temperature.[22] An increased cooling rate decreases the amount of proeutectoid ferrite that can form during transformation and, as a consequence, the time of transformation is reduced. The austenite grain size also plays an important role. As Lee *et al.*[21] concluded, the phase transformation of coarse-grained austenite was susceptible to cooling rate. Retained strain, on the other hand, tends to increase transformation rates and temperatures. However, this effect is strongly decreased for the higher cooling rates and finer austenite grain size. Niobium in solid solution lowers T_s in undeformed austenite, but raises it in the deformed condition. Precipitated niobium, on the other hand, accelerates the onset of the γ/α transformation (raises T_s), but retards the progress of transformation. The influence of chemical composition on the transformation start temperature was, therefore included in constant A in Eq. [3]. However, as concluded elsewhere,[16,17] at low strain, the decrease of T_s describes the hardenability properties of niobium in solution in austenite, which vanish at high strains.

III. AUSTENITE-TO-FERRITE TRANSFORMATION MODEL

After considering the analyses of existing models of austenite decomposition presented previously, we decided that

the method adopted in the present work would rely on isothermal transformation kinetics and the principle-of-additivity rule. It can be expected that if finite-element-method calculations are used, this model will give reasonably good results and, at the same time, will take into account all necessary thermodynamics requirements.

The model of austenite—ferrite transformation kinetics is based, in general, on a common Avrami–Johnson–Mehl equation. As previously mentioned, originally Umemoto *et al.*[26,27] proposed modification of the Avrami–Johnson–Mehl equation by including the effect of austenite grains size (Eq. [4]). The authors stated that when pearlite or ferrite forms from austenite by isothermal holding below the T_s temperature, these nuclei form preferentially at the prior-austenite grain boundary. However, this assumption is generally correct for continuous cooling conditions in lower ranges of cooling rates and for a refined austenite structure. Because such conditions meet most of the modern thermomechanical processes, this assumption was also considered in the present work. Umemoto *et al.*[26] proposed the following rate for ferrite and pearlite transformation, considering the kinetic laws derived by Cahn and Hagel[28] and taking into account the effect of austenite grain size:

$$X = 1 - \exp\left(-b\,\frac{t^n}{D_\gamma{}^m}\right) \qquad [4]$$

where X is the transformed fraction; t is an isothermal holding time; D_γ is the austenite grain size; b is the nucleation-and-growth rates constant, which depends only on transformation temperature; n is the parameter related to the geometry of the growing phase and the conditions of nucleation; and m is an constant.

In the present model, the γ-α transformation kinetics during continuous cooling had been derived from the isothermal conditions and by employing the additivity rule. However, the transformed fractions become precisely additive when one of the following conditions is satisfied: (1) the ratio of the nucleation rate and growth rate is invariant with temperature (isokinetic reaction), (2) all the nuclei have been nucleated early in the reaction and the progress of transformation is controlled only by their growth, and/or (3) the progress of transformation is controlled only by the nucleation of a new phase.

To determine the kinetic parameters n and b, the Avrami equation can be written as follows:

$$\ln\left(\ln\left(\frac{1}{1-X}\right)\right) = n \ln t + \ln b \qquad [5]$$

Using the previous equation, from a plot of ln (ln (1/(1 − X)) against ln t, the slope of the line gives the values of n and ln b (Campbell *et al.*[31]). A similar procedure can be used to estimate the value of the m parameter:

$$n \log t = m \log D_\gamma + \log\left(\ln\left(\frac{1}{1-X}\right)\right) - \log b \qquad [6]$$

Thus, when n is not a function of austenite grain size, the slope of the n log t *vs* log D_γ plot gives the value of m.[33] In the present work, the values of parameters m and n are close to 1.

The b constant in Eq. [4] is, in general, a kinetic parameter that represents the combination of nucleation and growth rates. For steels with a low carbon content, the value of parameter b can be calculated using either of the following equations (Howbolt *et al.*[33] and Cambell *et al.*[31]):

$$b = \exp\left(-0.25 \times 10^{-3} T^2 + 0.31\,T - 93.55\right) \qquad [7]$$

$$b = \exp\left(-0.0145\,\Delta T + 3.98 \ln \Delta T - 5.39\,(\text{pct C}) - 16.5\right) \qquad [8]$$

where ΔT is the undercooling below T_s.

The isothermal transformation kinetic is then employed to predict contunuous-cooling transformation using Scheil's additivity rule, assuming that the instantaneous transformation rate is a function only of the transformation temperature and already-transformed fraction X (Christian[34]).

$$\frac{dX}{dt} = \frac{H(T)}{G(X)} \qquad [9]$$

where $H(T)$ is a function of the temperature only, and $G(X)$ is a function of the fraction transformed.

The principle of additivity states that the transformation process is a series of isothermal events. The idea of analyzing the transformation kinetics adopted here is similar to that employed to predict the progress in austenite recrystallization under continuous cooling conditions.[35,36] Scheil[29,34,37] assumed that austenite consumes its fractional nucleation time and, when the sum of such fractions equal unity, the transformation starts:

$$\int_{t=0}^{t-t^n} \frac{dt}{\tau(T)} = \int_{T_e}^{T} \frac{dt}{dT} \cdot \frac{dT}{\tau(T)} \qquad \text{or} \qquad \int_0^t \frac{dt}{t_a(T)} = 1 \qquad [10]$$

where T_e and T are the cooling start and finish temperatures, respectively; $\tau(T)$ is the incubation time; t is the time; and $t_a(T)$ is the isothermal time to reach X_a.

The concept of additivity was also proposed to hold the incubation stage of a transformation. The incubation time can be derived from the experimental data using the growth equation (Zener[38])

$$\tau(T) = A\,\frac{\exp\left(\dfrac{Q}{RT}\right)}{\Delta T^u} \qquad [11]$$

where A and u are regression parameters.

However, as several works[37,39] concluded, it is difficult to obtain isothermal data for low-carbon steels because their incubation times are very short. Thus, in the present model, it is assumed that for the microalloyed steels, the austenite-ferrite decomposition starts immediately after achieving the transformation start temperature. Hence, extending Scheil's additivity rule (Eq. [10]) to the entire range of transformation (Tamura[29]), the incubation time ($\tau(T)$) is replaced with the time required for the reaction to reach a certain fractional completion (X) by isothermal holding at temperature (T).

The validity of the Scheil additivity rule for predicting the completion of the transformation event was examined in several works.[30,32,33] The authors concluded that only the transformation event could be described successfully by the Scheil equation. Thus, inclusion of the incubation period in the calculation leads to significant overestimation of continuous-cooling transformation kinetics. In spite of many criteria mentioned here and discussed widely elsewhere, the

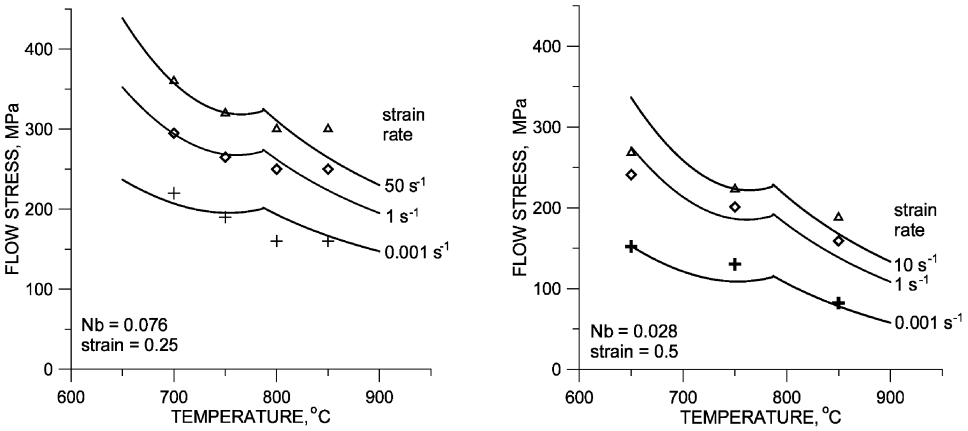

Fig. 1—Comparison of experimentally obtained and calculated (Eq. [17]) flow stress for various deformation conditions and niobium contents.

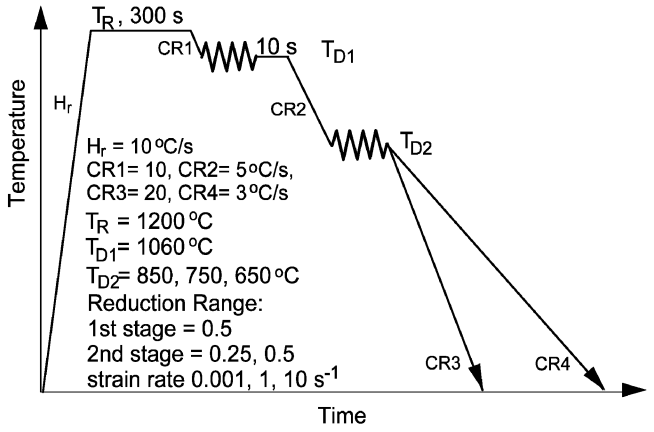

Fig. 2—Schematic representation of the thermomechanical treatment in two-stage Gleeble-simulator tests.

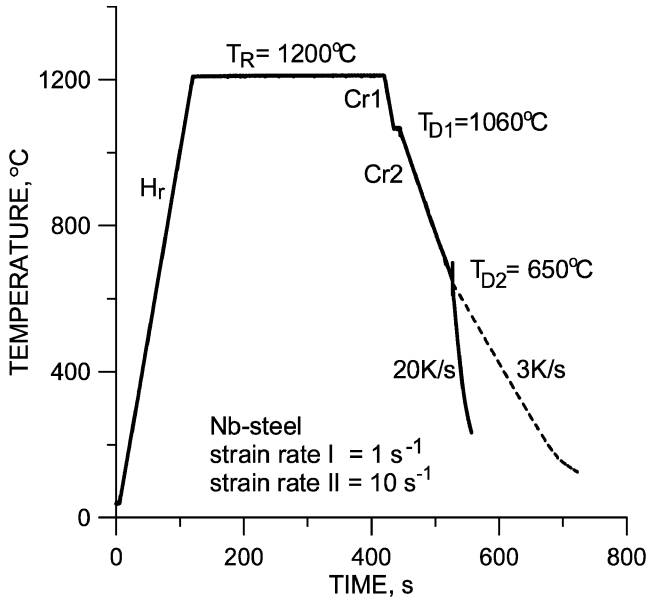

Fig. 3—Example of data collected during tests: T_R, T_{D1}, and T_{D2} reheating and first and second stage temperatures, respectively.

application of the additivity rule can be very useful. Hence, application of the idea proposed by Umemoto *et al.* and in later extensive works for the austenite-ferrite transformation during nonisothermal treatment, can be successfully employed in the modeling process.

Analysis of Heat Effect

Any successful application of the approach presented previously would require employing a model of heat generation during phase transformation. The present model was formulated for the case when heat transfer depends on different cooling conditions and the initial temperature distribution in the analyzed body is not uniform. Such an established model makes it possible to calculate and analyze all eventual differences in temperature distribution that can occur in hot-deformed material. The latent heat of the austenite-ferrite phase transformation varies, however, with temperature, because of the dependence of the specific heat on the particular phases. The enthalpy change for the austenite-ferrite transformation can be determined by integration of the difference of the austenite and ferrite heat capacities (Campbell *et al.*[30]):

$$\Delta H_i = \Delta H_l + \int_{T_l}^{T_i} (c_{p,\alpha} - c_{p,\gamma}) dT \qquad [12]$$

where ΔH_i and ΔH_l are enthalpy differences of ferrite and austenite at temperatures T_i and T_l, respectively; and $c_{p,\alpha}$ and $c_{p,\gamma}$ are the heat capacities of ferrite and austenite, respectively.

Employing linear or polynomial equations for the dependence of the enthalpy difference on temperature, Eq. [12] can be solved over a temperature range applicable to ferrite formation. Since the heat capacities of both ferrite and austenite do not depend on the carbon content,[40] in the present model, the following linear equation was employed to fit the published experimental data:[30,40]

$$\Delta H_i = 282 - 0.3\,T \qquad [13]$$

However, the enthalpy change for the ferrite transformation rises sharply between 740 °C and 780 °C, resulting from the ferromagnetic transition at 770 °C.

Thus, the total latent heat generated during the austenite-ferrite transformation can be calculated as a sum of heats

generated during a time step (Δt) of austenite decomposition, as follows:

$$Q = \rho \Delta H_i \frac{\Delta X}{\Delta t} \qquad [14]$$

where ρ is the density.

IV. FINITE-ELEMENT MODEL OF THE DEFORMATION AND HEAT TRANSFER

Plastometric tests, including the compression test, involve inhomogeneity of deformation. Therefore, an interpretation of the results of those tests presents some difficulties, which can be avoided when simulation of the tests is incorporated. The problem of inhomogeneity of microstructural development in hot-formed products is still not well understood. This may strongly affect a material's damage behavior. Monitoring the impact of the austenite-ferrite transformation process on the microstructural development and resulting mechanical properties under industrial conditions is difficult and expensive. The austenite decomposition model presented in this work could help to control the production processes in both off-line and on-line systems.

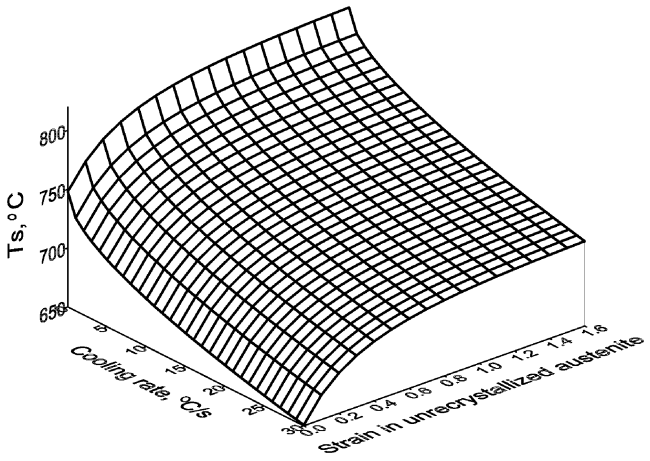

Fig. 4—Example of T_s calculation; austenite grain size $D_0 = 80$ μm.

The finite-element model is composed here of two parts. The first is the mechanical component, based on the rigid-plastic flow formulation, which computes the stresses,[41] strains, and strain rates during the deformation processes. This component is then coupled to a model of heat transfer during the experiment, based on the solution of a general convective diffusion equation.

The authors in References 42, 43 and 44 give a detailed description of the finite-element-method implementation where it is applied to the compression processes. Further application to the rolling is discussed in References 45 and 46. The aforementioned methods describe the flow stress in a material assuming the coexistence of the two phases—austenite and ferrite.

For the niobium-microalloyed steel, the flow stress can be described on a macroscopic scale as a function of the effective strain, effective strain rate, temperature, and carbon content. The flow stress for hot-forming processes has been extensively discussed in the literature. In the present work, for deformation temperatures below RST (recrystallization stop temperature), the modified equation originally suggested by Shida is employed.[43] The original equation does not require description of the coefficients; the only variable that represents the deformed material is the carbon-content equivalent. This equation, on the other hand, does not include effects of dynamic recrystalization, but it describes more accurately behavior of the material in a two-phase region.

Shida's equation, after modification for the niobium-treated microalloyed steels, can be described as follows:

$$\sigma = \sigma_f f \left(\frac{\dot{\varepsilon}}{z}\right)^m + (A_3(\text{pct Nb}) + A_4) \qquad [17]$$

where $\dot{\varepsilon}$ is the strain rate (pct Nb) is the niobium content

$$z = A_1 \dot{\varepsilon} + A_2; \quad A_1 = 6;$$

$$A_2 = 33; \quad A_3 = 1958; \quad A_4 = -70.8$$

$$q = 30(C_{eq} + 0.9)\left(t_T - 0.95 \frac{C_{eq} + 0.49}{C_{eq} + 0.42}\right)^2 + \frac{C_{eq} + 0.06}{C_{eq} + 0.09} \qquad [18]$$

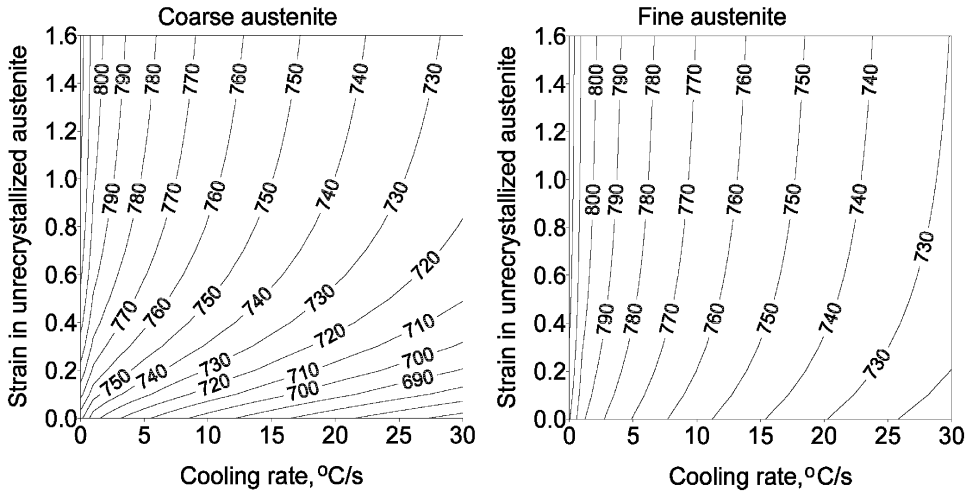

Fig. 5—Effect of the austenite structure at various cooling rates and retained strains on the austenite-ferrite transformation start temperature.

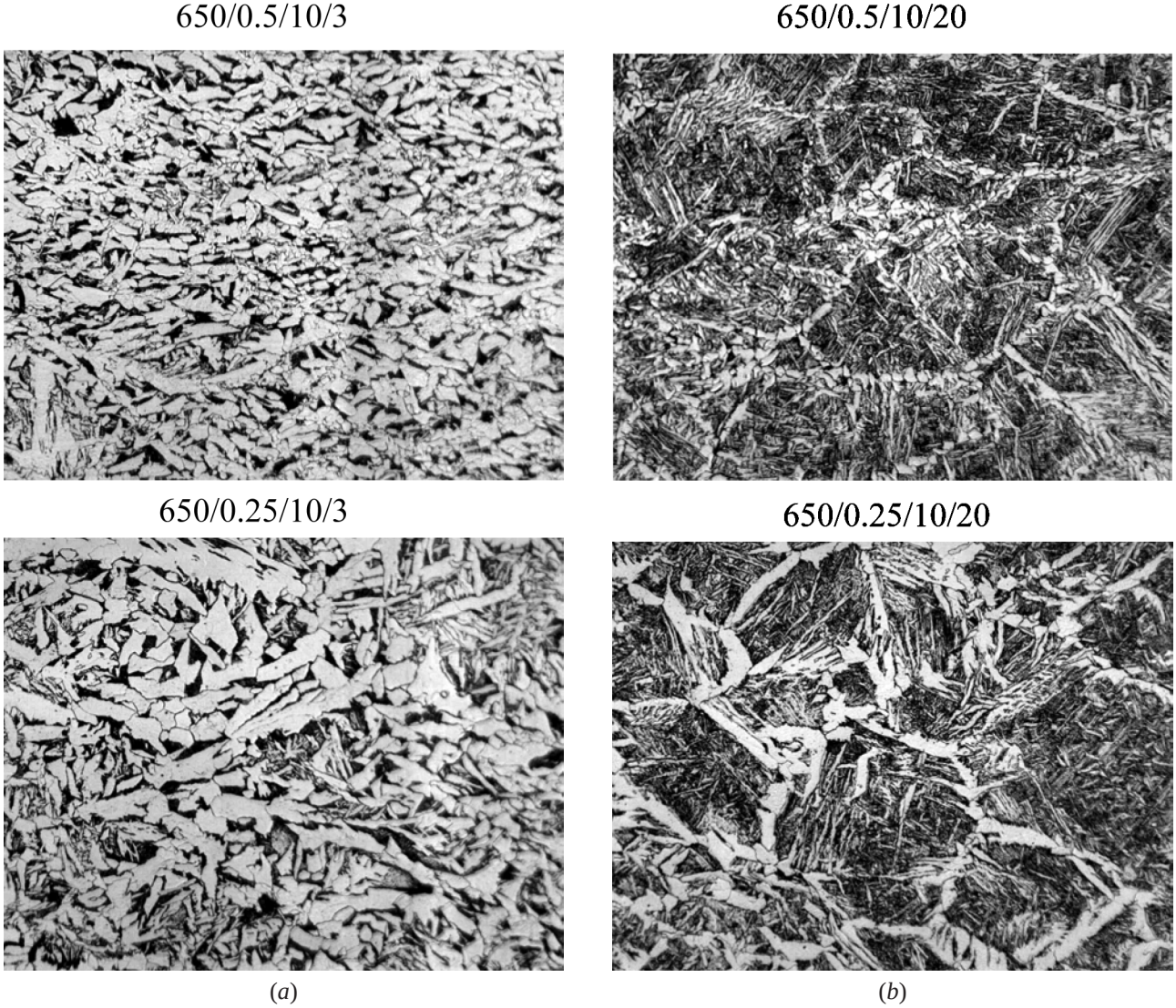

Fig. 6—(*a*) and (*b*) Optical microstructures obtained under various deformation conditions in the second stage of compression: T_{D2}/strain/strain rate/cooling rate.

$$t_T = \frac{T + 273}{1000}$$

In the case of deformation in the two-phase region,

$$t_T < \frac{T_s + 273}{1000} \quad [19]$$

$$\sigma_f = 0.28\ q \exp\left(\frac{C_{eq} + 0.32}{0.19(C_{eq} + 0.41)} - \frac{0.01}{C_{eq} + 0.05}\right) \quad [20]$$

$$m = (0.081\ C_{eq} - 0.154)t_T - 0.019\ C_{eq} + 0.207 + \frac{0.027}{C_{eq} + 0.32} \quad [21]$$

The other parameters are defined as:

$$f = 1.3(5\ \varepsilon_i)^n - 1.5\ \varepsilon_i \quad [22]$$

Where ε_i is the natural strain, C_{eq} is the carbon equivalent, and $n = 0.41 - 0.07\ C_{eq}$.

In formulating the flow stress of niobium-microalloyed steels at elevated temperatures, especially in the two-phase region, the question is which of the process parameters is the most important factor in the formula. Taking into account formula [3], which describes the beginning of the austenite decomposition process, the basic parameters of the deformation and microstructural development processes can be employed in Eqs. [17] and [19].

The characteristic feature of the aforementioned approach is the possibility of calculating the flow stress not only in the austenite, but also in the austenite-ferrite two-phase region. The comparison of calculated and measured flow stresses is presented in Figure 1. Here, the experimental results of previous works have been used as well.[18,24,25,43]

V. THE EXPERIMENTAL ASSESSMENT OF THE AUSTENITE-FERRITE TRANSFORMATION MODELING

Results presented in this work were obtained in hot-compression tests performed in austenite and austenite-ferrite regions with various deformation conditions, using a Gleeble 1500/20 thermomechanical simulator. The effects of the

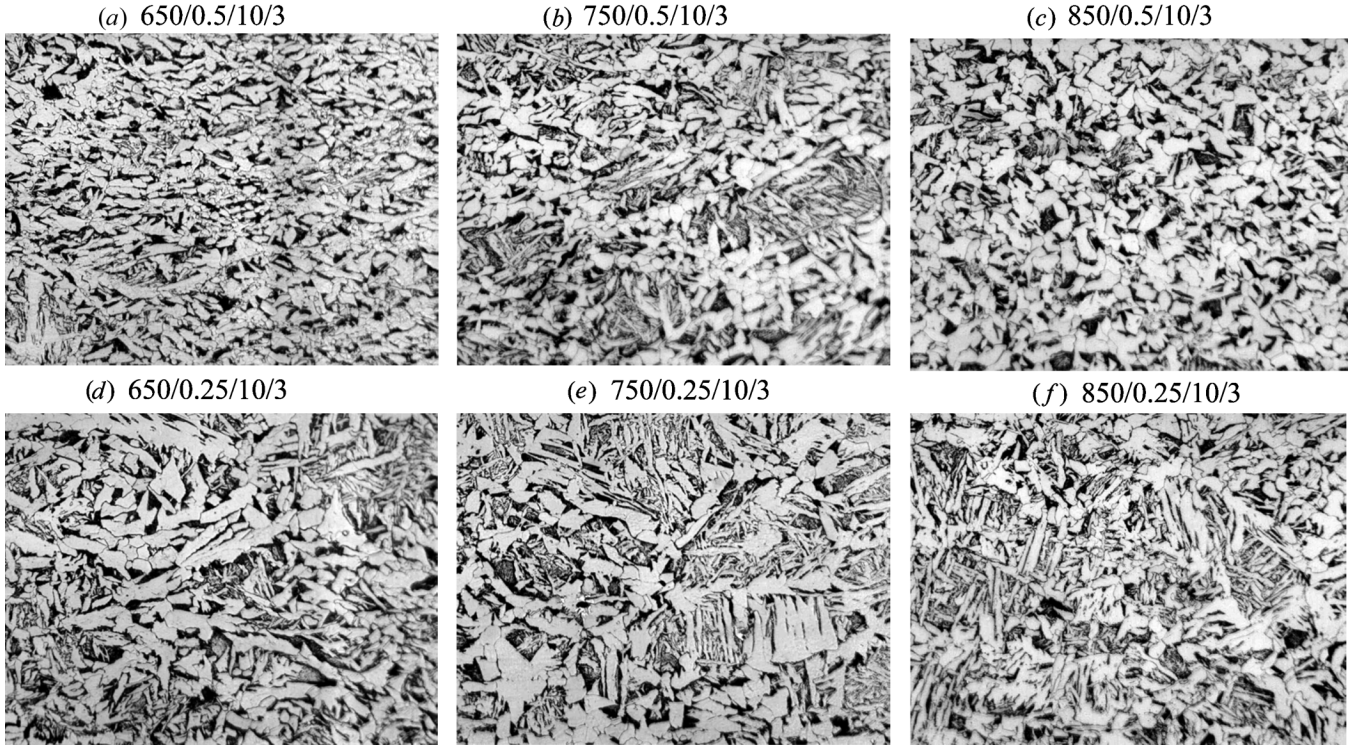

Fig. 7—(*a*) through (*f*) Optical microstructures obtained under various deformation conditions in the second stage of compression: T_{D2}/strain/strain rate/cooling rate.

deformation in the two-phase region are discussed in relation to the microstructural development, austenite-to-ferrite phase transformation, and final ferrite-pearlite structure of niobium-treated microalloyed steel. The heating and deformation conditions are shown schematically in Figure 2. Figure 3 presents examples of temperature *vs* time data collected during tests. The chemical composition of the tested steel is 0.09 C/1.55 Mn/0.31 Si/0.028 Nb/0.01 V. The procedure for experiment preparation was as follows. First, chromel-alumel thermocouples were capacitor-discharge welded at the specimen's midheight point on its outer-diameter surface before testing. Specimens were held and heated between tungsten carbide (WC) platens. The platens were first coated with a thin film of molybdenum powder dissolved in water for the purpose of lubrication. Next, a 0.003-in.-thick tantalum sheet was placed between the specimen and a dynamic vacuum was maintained throughout the testing. Controlled cooling steps were accomplished by purging with helium in the testing zone. All specimens were analyzed using optical microscopy. In particular, the coupled effects of temperature, strain, strain rate, and cooling rate on the resulting microstructure were analyzed.

VI. RESULTS AND DISCUSSION

A. *Transformation Start Temperature*

The first element in characterization of microstructural development, which can be affected by austenite hardening, is the austenite-to-ferrite transformation start temperature (T_s). In the present work, it was assumed that the ferrite transformation starts when the temperature drops to the equilibrium temperature (T_s). Thus, considering the effect of the stored energy in the unrecrystallized austenite, we stated that the transformation start temperature depends mainly on the cooling rate, austenite grain size, and retained strain. Using all experimental data obtained, we propose that the transformation start temperature can be reasonably well calculated according to the previously presented Eq. [3]. The examples of the calculations of the T_s temperature are presented in Figures 4 and 5.

B. *Role of Niobium*

The niobium addition is one of the most effective microalloying elements in modern thermomechnically treated steels. So, in the discussion about austenite decomposition, special attention should be focused on this element. Precipitates of carbides, nitrides, or carbonitrides in the austenite phase inhibit recrystallization of the austenite. This leads directly to ferrite refinement after transformation of unrecrystallized austenite. The effect of steel chemical composition on the transformation kinetics has obvious importance in relation to both ferrite nucleation and growth. The role of niobium precipitates on austenite decomposition was estimated differently in the literature. Precipitates in austenite can accelerate the γ/α transformation because they act as potential nucleation sites and raise the T_s temperature. As Lee *et al.*[47] suggest, solute niobium strongly segregates to the γ/α phase boundary and reduces ferrite growth kinetics because of the solute drag effect and, thus, lowers the T_s temperature. However, the quantitative relationship between solute niobium and the lowering of the T_s temperature are not in agreement. Another consequence of precipitation in austenite is that less niobium is left in solution, which decreases the ability of austenite to harden and promotes the occurrence

of the γ/α transformation. On the other hand, when the niobium is still in solution during phase transformation, new precipitates form on the γ/α interfaces, which significantly decrease the interface mobility and retard the progress of transformation. In that case, the precipitation slows down the transformation. Ouchi *et al.*[16] clearly show that a small amount of niobium appreciably retards the ferrite nucleation rate. Because the alloying amount of niobium is usually small, niobium does not seem to alter the free-energy change during transformation to a great extent. In addition, they reported that the solute niobium exerts a large influence on the ferrite-austenite phase boundary and that the solute niobium on and near the grain boundary lowers the γ grain-boundary energy, thus lowering the nucleation rate of ferrite. If such is the case, the nucleation rate will be rapidly increased when the interfacial energy of the austenite grain boundary is raised. This is because a decrease in solute niobium is caused by the strain-induced precipitation.

The aforementioned issues concerning niobium in microalloyed steels were included in the present model. In consequence, a new quality of the modeling of the development of microstructure was obtained, and a full, real-life kinetics of the austenite-ferrite transformation is accounted for.

C. *Microstructural Development*

Examples of microstructures obtained under various deformation conditions are shown in Figure 6. Here, particular conditions of the experiment, *i.e.*, the temperature T_{D2}, strain, strain rate of the second stage of deformation, and cooling rate (between the temperatures T_s and 600 °C) are presented. It is clear, for both cooling rates presented here, that increasing strain involves structure refinement (Figures 6(a) and (b)).

The influence of deformation temperature and strain on the ferrite microstructure is shown in Figure 7. Significant refinement can be observed in all cases of deformation temperature, when the strain increases. Decreasing the deformation-stored energy (a higher deformation temperature supports the restoration process) favors bainite formation (Figures 7(d) through (f)). This effect is especially pronounced in the case of coarse austenite. After deformation in the two-phase region, the inhomogeneity of the resultant structure increases. Any successful application of the approach mentioned previously would require employing a model of heat generation during phase transformation. The present model was formulated for the case when heat transfer depends on different cooling conditions and the initial temperature distribution in the analyzed body is not uniform. Such an established model makes it possible to calculate and analyze all eventual differences in temperature distribution that can occur in hot-deformed material. Therefore, the latent heat of the austenite-to-ferrite phase transformation varies with temperature because of the dependence of specific heat on the particular phases. In the present model, as mentioned earlier, the γ-α transformation kinetics during continuous cooling were derived from the isothermal conditions and by employing the additivity rule.

Figure 8 shows the flow curves of analyzed steel for various finish deformation temperatures and strain rates (refer to the experimental procedure shown in Figure 2). The appearance of these flow curves is typical for deformation in

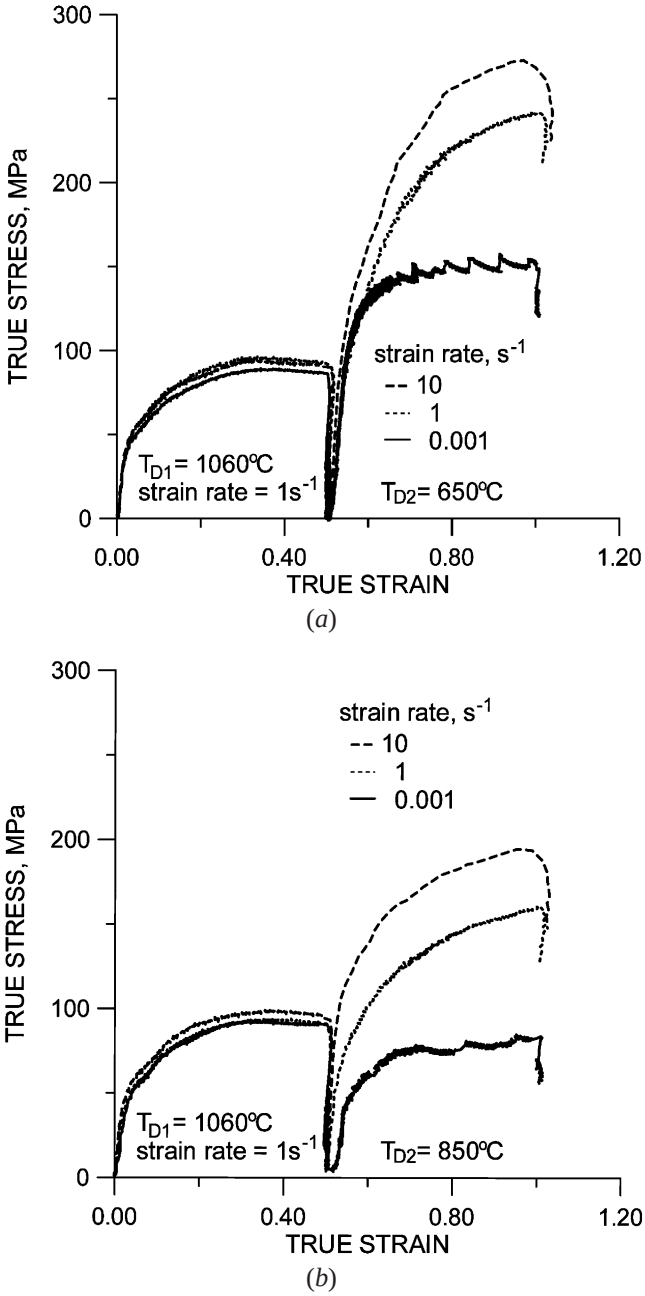

Fig. 8—Flow curves obtained with different finish deformation temperatures and strain rates: (*a*) T_{D2} = 650 °C and (*b*) T_{D2} = 850 °C.

the two-phase region. Increasing the strain rate involves an increase in flow stress similar to the influence of decreasing deformation temperature. However, the resulting final microstructure reflects different features. Thus, the changes in the transformed microstructure are controlled by the cooling rate. Analyses of the optical micrographs showed that the influence of the cooling rate and amount of deformation are similar to those obtained under typical conditions, *i.e.*, when finish deformation occurs in the austenite phase (Figure 7). It is also observed that when the cooling rate increases, the pearlite is replaced by an increased amount of finely dispersed bainite. The niobium-microalloyed steels exhibit a very strong tendency to bainite formation, in particular for the coarse austenite structure. Experimental and modeling results showed that bainite formation recedes by

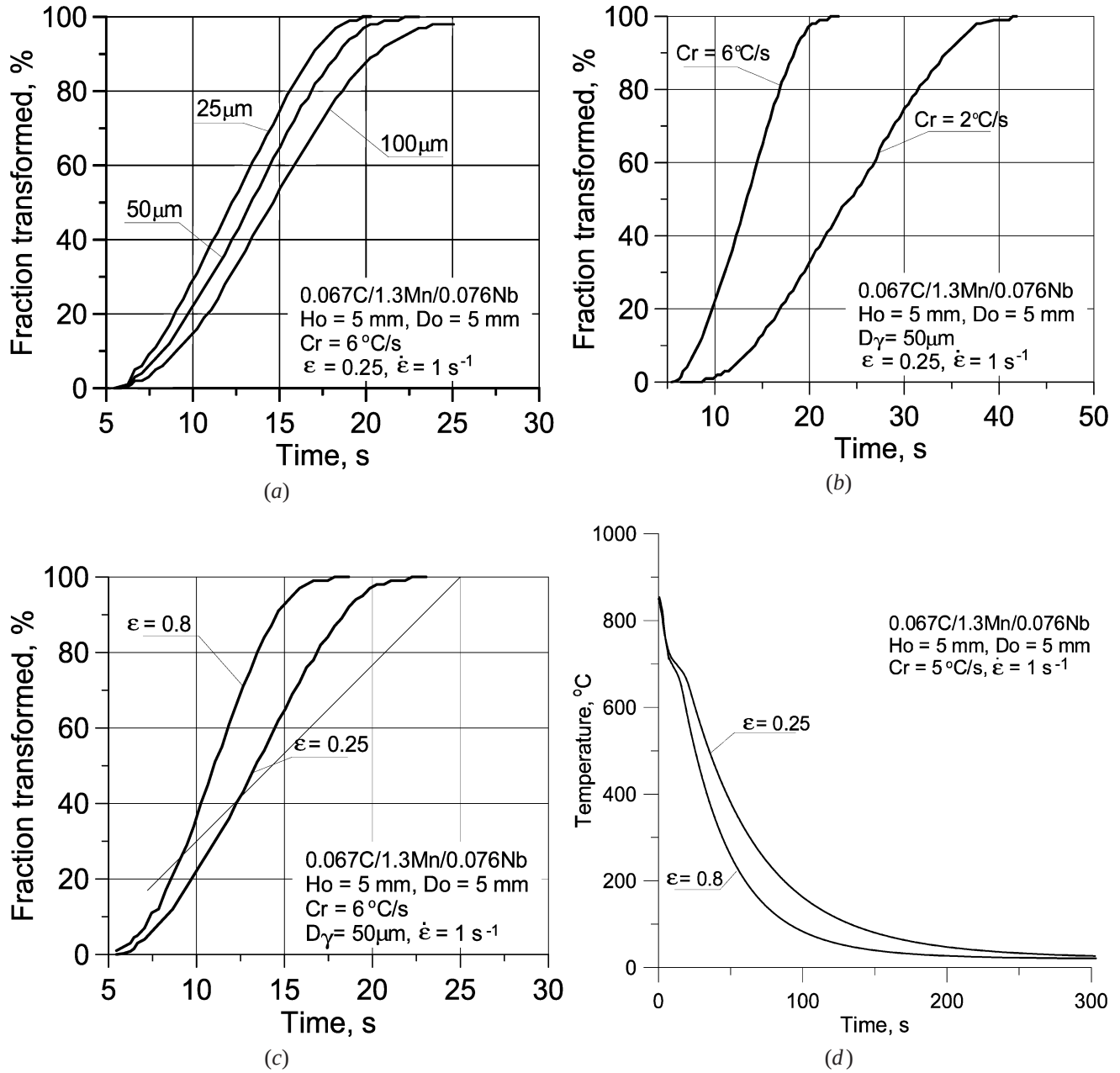

Fig. 9—Example of calculations. Influence of the deformation and microstructure parameters on the fraction transformed: (*a*) austenite grain size, (*b*) cooling rate, and (*c*) strain. (*d*) Cooling curve for various amounts of deformation.

an increase in deformation preceding phase transformation under constant strain rate and temperature (Figure 7). The exact evaluation of the contents of a particular phase, however, needs further work. In the case of lower cooling rates (3 K s^{-1}), conditions of the final microstructure are more obvious and could be calculated reasonably accurately. Examples of implementation of the austenite-ferrite transformation model are shown in Figure 9. The presented results reflect all of the important characteristic behaviors. The calculated cooling curve is presented in this figure. The cooling curves shown in Figure 10 prove that the austenite refinement accelerates the transformation kinetic. In addition, an increasing cooling rate increases progress of the transformation kinetic.

Finally, using the analysis of the obtained microstructures, the comparison between calculated and measured transformed fractions is presented in Figure 11 and shows that the calculated results for the austenite decomposition model are in correct agreement with the experiment. The next example of calculations for the present experimental conditions is presented in Figure 12.

The proposed model makes it possible to take into account the initial austenite microstructure, as well as the deformation conditions. As mentioned earlier, knowledge of the transformed fraction enables us to calculate the distribution of effective strain in particular phases. Figure 13 presents examples of calculations for the compression process in the two-phase region. The influence of the initial inhomogeneity on the amount of the effective strain accumulated in the specimens deformed at various temperatures is well

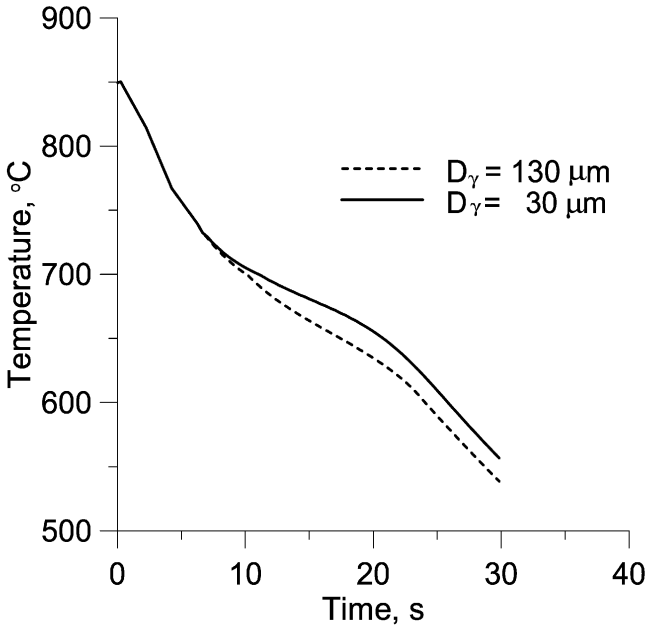

(*a*)

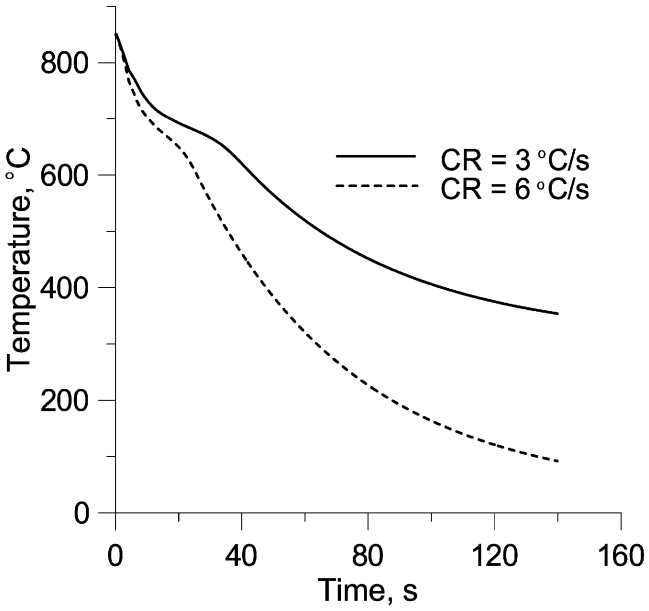

(*b*)

Fig. 10—Example of calculations. Effects of the austenite grain size (*a*) and cooling rate (*b*) on the cooling curves. CR = average cooling rate in the range of temperature 650 ÷ 55 °C.

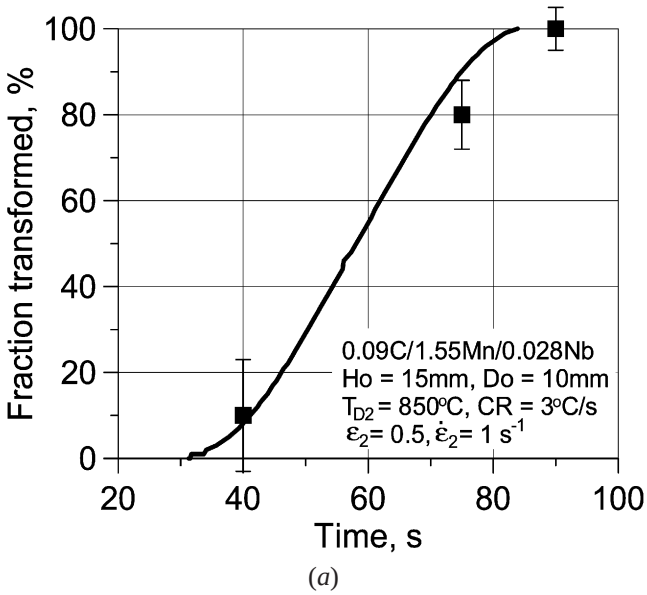

(*a*)

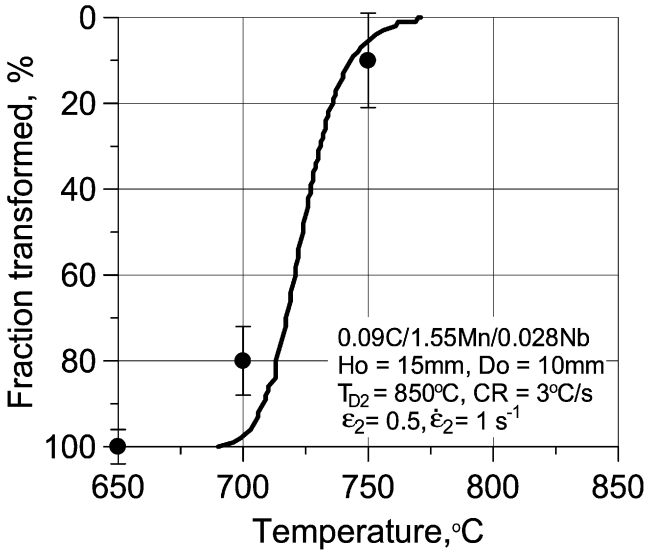

(*b*)

Fig. 11—Example of calculations. Fraction transformed *vs* (*a*) time and (*b*) temperature.

reflected. As a result, the complete history of microstructural development can be analyzed, even in such complex conditions as a deformation in the two-phase region.

After deformation in the two-phase region, the inhomogeneity of the resultant structure increases. The source of such inhomogeneity is the effective strain distribution (Figure 13). However, differences in descriptions of austenite decomposition kinetics also play a significant role here.

VII. SUMMARY AND CONCLUSIONS

The austenite decomposition model proposed makes it possible to calculate microstructural phenomena as a part of the simulation of hot-working processes and to determine final inhomogeneity dependent on the thermomechanical materials history. Special attention was given to the description of the influence of finish deformation temperature and strain rate on the austenite-to-ferrite transformation process. A new idea for the phase transformation start temperature is also proposed. Existing models of austenite decomposition kinetics were extensively reviewed. As a result, particular components of the transformation model were determined. The presented model effectively links the advanced finite-element approach simulating metal flow and heat transfer during hot plastic deformation with the submodels describing microstructural development and phase-transformation mechanisms. Results of the computer simulations are compared with those obtained experimentally. The axisymmetrical compression-test experiments were used to evaluate the effects of deformation in austenite and the two-phase region on the microstructural development. Hence, the influence

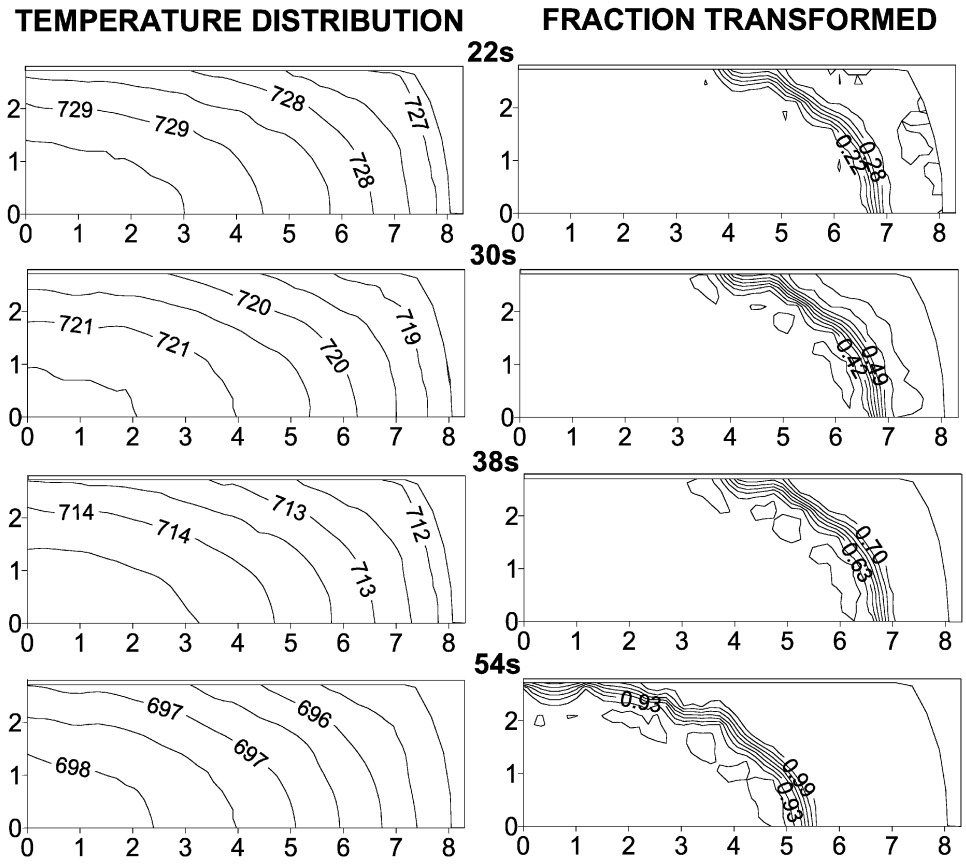

Fig. 12—Example of calculations. Distributions of temperature and fraction transformed in the specimens deformed at T_{D2} = 850 after marked cooling time. Strain = 0.5, strain rate = 1 s^{-1}, stage 2.

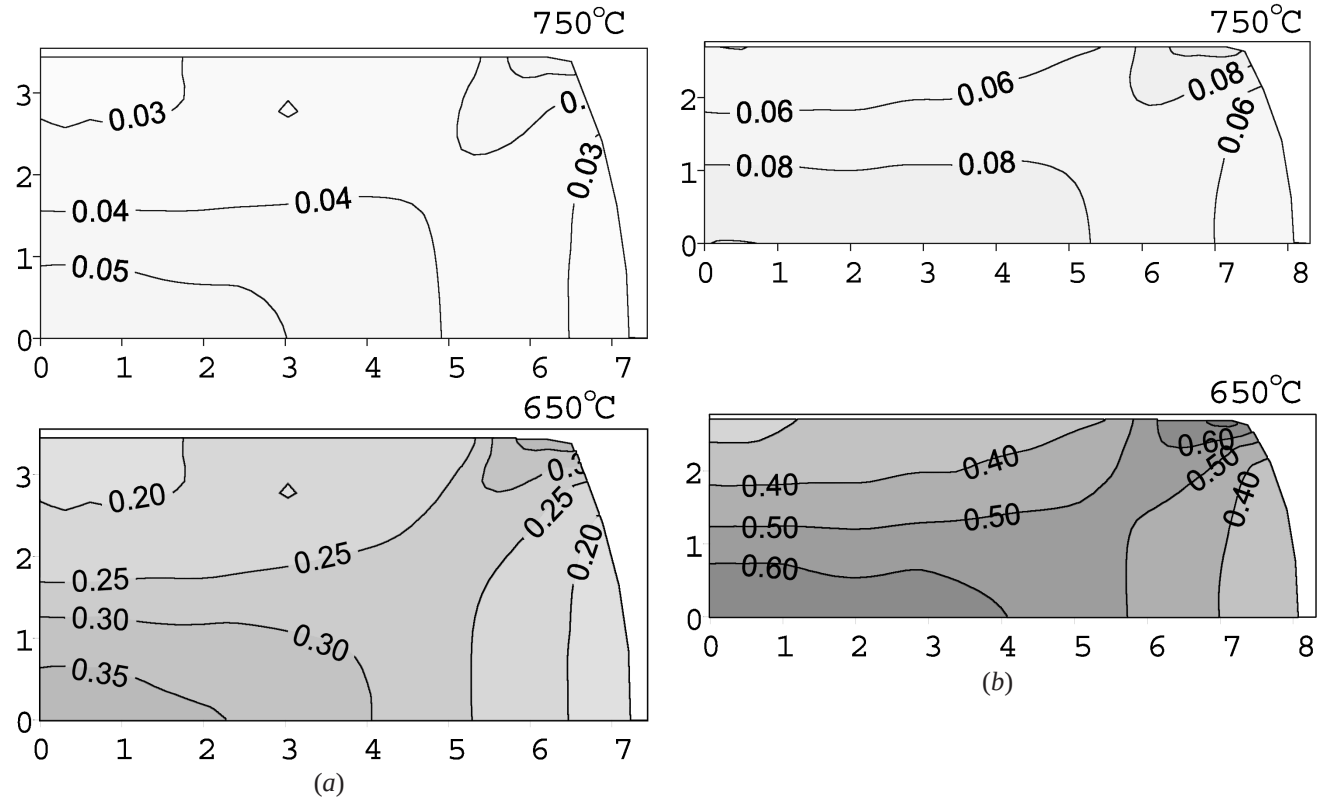

Fig. 13—Example of calculations. Distributions of effective strain in ferrite phase after second deformation with strain (*a*) 0.25 and (*b*) 0.5. Strain rate = 1 s, stage 2.

of the deformation conditions (temperature, strain rate, *etc.*) on the phase transformation and final microstructure and inhomogeneity were analyzed. It is concluded that the changes in ferrite structure are the result of the deformation conditions, *i.e.*, strain rate and amount of strain, as well as cooling rate. Good correspondence between the experimental and simulated data confirmed correct construction of the phase-transformation model and its effectiveness in hot-working processes of Nb-microalloyed steels. The scope of this work proved the possibilities of using computer modeling to design modern steels and processes. Finally, because of the complexity of the problems mentioned, further study in this area is necessary before significant progress can be made.

The following main conclusions are drawn from the present study.

1. It is possible to describe qualitatively the kinetics of the austenite-to-ferrite transformation and the resulting structure development in niobium-microalloyed steel. Such a description represents a modern tool particularly useful in the modification of existing or newly developing technologies for thermomechanical warm- and hot-working processes, with emphasis on the properties of final product optimization. The results obtained using the proposed transformation model are especially useful in an exact analysis and description of microstructural development in the two-phase region.
2. Experimental and modeling results showed that bainite formation recedes by an increase in deformation preceding phase transformation under constant strain rate and temperature.

ACKNOWLEDGMENTS

The financial support of the Maria Sklodowska-Curie Fund II (Grant No. MEN/DOE-97-315) and Polish Committee for Scientific Research (Research Project AGH No. 11.11.110.117) are gratefully acknowledged. The authors thank Dan Thoma, Los Alamos National Laboratory, for performing dilatometric tests.

REFERENCES

1. C.M. Sellars and J.H. Beynon: in *High Strength Low Alloy Steels*, D.P. Dunne and T. Chandra, eds., University of Wollongong, Wollongong, NSW, 1984, pp. 142-50.
2. P.C. Campbell, E.B. Hawbolt, and J.K. Brimacombe: *Metall. Trans. A*, 1991, vol. 22A, pp. 2791-2805.
3. J.S. Kirkaldy: *Metall. Trans.*, 1973, vol. 4, pp. 2327-33.
4. M. Suehiro, H. Yada, T. Senuma, and K. Sato: *Proc. Int. Conf. Mathematical Modeling of Hot Rolling of Steel*, S. Yue, ed., CIMM, Hamilton, 1990, pp. 128-37.
5. M. Suehiro, T. Senuma, and H. Yada: *Tetsu-to-Hagane*, 1987, vol. 73, pp. 1026-32.
6. T. Senuma, M. Suehiro, and H. Yada: *Iron Steel Inst. Jpn. Int.*, 1992, vol. 32 (3), pp. 423-32.
7. S. Torizuka, N. Ohkouchi, T. Minote, M. Niikura, and C. Ouchi: *Thermomechanical Processing in Theory, Modelling & Practice*, B. Hutchinson, M. Andersson, G. Engberg, B. Karlsson, and T. Siwecki, eds., Sweden, 1996, pp. 227-39.
8. Yoshie, M. Fujioka, Y. Watanabe, K. Nishioka, and H. Morikawa: *Iron Steel Inst. Jpn. Int.*, 1992, vol. 32 (3), pp. 395-404.
9. P. Choquet, P. Fareque, J. Giusti, B. Chamont, J.N. Pezant, and F. Blanchet: *Mathematical Modeling of Hot Rolling of Steel*, S. Yue, ed., CIMM, Hamilton, Canada, 1990, pp. 34-44.
10. S. Kamamoto, T. Nishimori, and S. Kinoshita: *Mater. Sci. Technol.*, 1985, vol. 1, pp. 798-804.
11. I. Boyadjiev, P.F. Thomson, and Y.C. Lam: *THERMEC 97*, T. Chandra and T. Sakai, eds., TMS, Warrendale, PA, 1997, pp. 2023-29.
12. I. Boyadjiev, P.F. Thomson, and Y.C. Lam: *Iron Steel Inst. Jpn. Int.*, 1996, vol. 36 (11), pp. 1413-19.
13. M. Umemoto, A. Hiramatsu, A. Moriya, T. Watanabe, S. Nanba, N. Nakajjima, G. Anan, and Y. Higo: *Iron Steel Inst. Jpn. Int.*, 1992, vol. 32 (3), pp. 306-15.
14. M. Umemoto: *Proc. Int. Symp. Mathematical Modeling of Hot Rolling of Steel*, S. Yue, ed., CIMM, Hamilton, 1990, pp. 404-12.
15. M. Umemoto, N. Komatsubara, and I. Tamura: *J. Heat Treating*, vol. 1, 1980, pp. 57-64.
16. C. Ouchi, T. Sampei, and I. Kozasu: *Trans. Iron Steel Inst. Jpn.*, 1982, vol. 22, pp. 214-22.
17. M. Piette and C. Perdrix: *Mater. Sci. Forum*, 1998, vol. 284-86, 361-68.
18. J. Majta, A.K. Zurek, and M. Pietrzyk: *Recrystallization '99*, JIMIS-10, Tsukuba Science City, Japan, 1999, pp. 691-96.
19. T. Tanaka: *Int. Met. Rev.*, 1981, vol. 4, pp. 185-212.
20. T. Gladman: *The Physical Metallurgy of Microalloyed Steels*, The Institute of Materials, London, 1997.
21. J.L. Lee, C.C. Yang, and I.C. Hsuan: *THERMEC 97*, T. Chandra and T. Sakai, eds., TMS, Warrendale, PA, 1997, pp. 451-57.
22. M. Militzer, W.P. Sun, W.J. Poole, and P. Purtscher: *THERMEC 97*, T. Chandra and T. Sakai, eds., TMS, Warrendale, PA, 1997, pp. 2093-99.
23. T. Tanaka and N. Tabata: *Tetsu-to-Hagane*, 1978, vol. 64, pp. 1353-62.
24. J. Majta, A.K. Zurek, and M. Pietrzyk: *J. Phys. IV France*, 1997, vol. 7 (C3), pp. 397-402.
25. A.K. Zurek and J. Majta: *7th Int. Symp. on Plasticity and Current Applications*, Cancun, Mexico, 1999, pp. 659-62.
26. M. Umemoto, N. Komatsubara, and I. Tamura: *J. Heat Treating*, 1980, vol. 1 (3), pp. 57-64.
27. M. Umemoto, K. Horiuchi, and I. Tamura: *Trans. Iron Steel Inst. Jpn.*, 1982, vol. 22, pp. 854-61.
28. J.W. Cahn and W.C. Hagel: *Acta Metall.*, 1963, vol. 11, p. 561.
29. I. Tamura: *Trans. Iron Steel Inst. Jpn.*, 1987, vol. 27, pp. 763-79.
30. P.C. Campbell, E.B. Hawbolt, and J.K. Brimacombe: *Metall. Trans. A*, 1991, vol. 22A, pp. 2791-805.
31. P.C. Campbell, E.B. Hawbolt, and J.K. Brimacombe: *Metall. Trans. A*, 1991, vol. 22A, pp. 2779-90.
32. M.B. Kuban, R. Jayaraman, E.B. Hawbolt, and J.K. Brimacombe: *Metall. Trans. A*, 1986, vol. 17A, pp. 1493-1503.
33. E.B. Hawbolt, B. Chau, and J.K. Brimacombe: *Metall. Trans. A*, 1985, vol. 16A, pp. 565-78.
34. J.W. Christian: *The Theory of Transformations in Metals and Alloys*, Pergamon Press, Oxford, United Kingdom, 1965, vol. 21, pp. 471-95.
35. J. Majta, J.G. Lenard, and M. Pietrzyk: *Metall. Foundry Eng.*, 1995, vol. 21, pp. 9-37.
36. J. Majta, J.G. Lenard, and M. Pietrzyk: *Mater. Sci. Eng.*, 1996, vol. 208, pp. 249-59.
37. I.A. Wierszyllowski: *Metall. Trans. A*, 1991, vol. 22A, pp. 993-99.
38. C. Zener: *Trans. AIME*, 1946, vol. 167, pp. 550-95.
39. J.J. Eber and W. Bleck: *Proc. Modeling of Metal Rolling Processes*, J.H. Beynon, P. Ingham, H. Teichert, and K. Waterson, eds., The Institute of Materials, London, 1996, pp. 185-90.
40. G.P. Krielaart, C.M. Brakman, and S. Van der Zwaag: *J. Mater. Sci.*, 1996, vol. 31, pp. 1501-08.
41. C.H. Lee and S. Kobayashi: *ASME, J. Eng. Ind.*, 1973, vol. 95, pp. 63-78.
42. M. Pietrzyk and J.G. Lenard: *Thermal Mechanical Modeling of the Flat Rolling Process*, Springer-Verlag, Berlin, 1991.
43. J. Majta, R. Kuziak, and M. Pietrzyk: *J. Mater. Processing Technol.*, 1998, vol. 80-81, 524-30.
44. A.K. Zurek, J. Majta, and M. Pietrzyk: *39th Mechanical Working and Steel Processing Conf.*, Conf. Proc. ISS, (ISS, Indianapolis, IN, 1998), vol. XXXV, pp. 577-82.
45. J. Majta, M. Pietrzyk, J.G. Lenard, and J. Jansen: *37th Mechanical Working and Steel Processing Conf.*, ISS, Hamilton, Canada, 1995, vol. XXXIII, pp. 89-99.
46. J. Majta, P. Munther, J.G. Lenard, Z. Kedzierski, and M. Pietrzyk: *5th ICTP*, Columbus, Ohio, USA, 1996, pp. 19-22.
47. K.J. Lee, K.B. Kang, J.K. Lee, O. Kwon, and R.W. Chang: *Proc. Int. Symp. Mathematical Modeling of Hot Rolling of Steel*, S. Yue, ed., CIMM, Hamilton, Canada, 1990, pp. 435-43.